Princeton Plasma Physics Laboratory

PPPL- 4827

PPPL- 4827

Comparison of Gas Puff Imaging Data in NSTX with the DEGAS 2 Simulation

B. Cao, D.P. Stotler, S.J. Zweben, M. Bell, A. Diallo and B. Leblanc

October, 2012

PPPL PRINCETON PLASMA PHYSICS LABORATORY

Prepared for the U.S. Department of Energy under Contract DE-AC02-09CH11466.

Princeton Plasma Physics Laboratory
Report Disclaimers

Full Legal Disclaimer

Trademark Disclaimer

PPPL Report Availability

Princeton Plasma Physics Laboratory:

http://www.pppl.gov/techreports.cfm

Office of Scientific and Technical Information (OSTI):

http://www.osti.gov/bridge

Related Links:

U.S. Department of Energy

Office of Scientific and Technical Information

Fusion Links

Comparison of gas puff imaging data in NSTX with DEGAS 2 simulations

B. Cao[1], D.P. Stotler[2], S.J. Zweben[2], M. Bell[2], A.Diallo[2], B. LeBlanc[2]

[1]*Institute of Plasma Physics Chinese Academy of Sciences, Hefei 230031, China*

[2]*Princeton Plasma Physics Laboratory, PO Box 451, Princeton, NJ, 08540 USA*

Abstract

Gas-Puff-Imaging (GPI) is a two dimensional diagnostic which measures the edge D_α light emission from a neutral D_2 gas puff nears the outer mid-plane of NSTX. DEGAS 2 is a 3-D Monte Carlo code used to model neutral transport and atomic physics in tokamak plasmas. In this paper we compare measurements of the D_α light emission obtained by GPI on NSTX with DEGAS 2 simulations of D_α light emission for specific experiments. Both the simulated spatial distribution and absolute intensity of the D_α light emission agree well with the experimental data obtained between ELMs in H-mode.

1. Introduction

The purpose of this paper is to compare the measured D_α light emission from a puff of neutral deuterium gas at the edge of NSTX with neutral particle simulations performed with the DEGAS 2 modeling code [1]. This comparison provides an improved validation of the DEGAS 2 code for deuterium, and also yields additional insight into the data from NSTX gas puff imaging (GPI) experiments.

In general, neutral deuterium plays an important role in tokamaks because it provides the source of fuel for the discharge. However, deuterium neutrals can also affect the energy balance of the plasma through radiation and charge exchange (CX), and can in theory produce damping of the edge momentum through CX collisions [2]. Neutrals can

enter the discharge from various sources: gas puffing from valves at the wall, recycling of deuterium from the wall, neutral beam injection, or pellet injection. The present paper considers only the deuterium gas puff source associated with the gas puff imaging diagnostic (GPI) on NSTX.

The absolute value and radial profiles of the neutral deuterium density from recycling in the main chamber have been measured previously on several tokamaks. Measurements on TEXT were made using a diagnostic neutral beam, a scanning neutral particle analyzer, and H_α detectors, and inferred neutral deuterium densities were ~10^9 cm^{-3} in the plasma center and ~10^{11} cm^{-3} at the edge [3]. Measurements of edge neutral deuterium on Alcator C-Mod were made using Lyman alpha emission with inferred neutral densities in the range $3x10^9$-$3x10^{11}$ cm^{-3} within ±3 cm of the separatrix in an Ohmic discharge [4]. More recently, the spatial distribution of D_α light emission was measured in ASDEX Upgrade using a calibrated camera, and neutral densities in the range 0.5-1 $x10^{10}$ cm^{-3} were found near the separatrix [5]. No measurements of neutral deuterium density in NSTX have been published, although an attempt was made to measure the neutrals using a camera with a D_β filter [6]. In Refs. [3-5], to obtain the local neutral density it was necessary to use the plasma density and temperature profiles to interpret the line emission brightness, and to reconstruct the local emission from the sightline line-averaged measurements.

In the present paper we do not measure the recycling light but instead measure the D_α brightness of the deuterium gas puff used for the gas puff imaging diagnostic (GPI) on NSTX [7-9]. This puff is similar to a fueling gas puff in that it is located at the outer midplane, triggered during a plasma discharge, and puffs D_2 gas at room temperature into the chamber. Although the D_α light from this GPI gas puff is much larger than the local D_α recycling light, it is smaller in magnitude than a fueling puff and does not significantly affect the line-averaged density or edge plasma parameters.

In this paper the measured D_α brightness from this GPI gas puff is compared with the DEGAS 2 neutral transport code [1] simulations. The initial study of GPI with DEGAS 2 was for deuterium in Alcator C-Mod [10]. That paper described how the D_α brightness

was expected to vary with assumed spatial fluctuations in the local density and temperature, and showed that excited atoms generated by molecular dissociation are a significant source of D_α photons. A second paper described DEGAS 2 modeling of helium GPI in NSTX [11], and showed that the radial width of calculated HeI brightness was in rough agreement with the GPI experimental results. That simulation also indicated that the finite extent of gas puff along the viewing direction did not significantly degrade the radial resolution of diagnostic, and provided a procedure to estimate the effective neutral density by comparing the simulation and GPI experiment. In a third paper on the analysis of GPI using DEGAS 2, the time response of HeI line emission to plasma density and temperature fluctuations was estimated to be ≤ 1 μsec [12], short enough to allow the conventional atomic physics model to be used when interpreting GPI experiments. That paper also showed that the calculated 2-D spatial emission profiles of HeI from DEGAS 2 matched well with the observed GPI in NSTX. Comparisons of the radial profiles of D_α emission between GPI and DEGAS 2 was also presented for Alcator C-Mod in [8] and for HeI emission for NSTX in [9].

In this paper we compare the 2-D spatial profile and absolute brightness of the deuterium D_α line emission from a GPI gas puff with DEGAS 2 simulations. This provides a substantial validation of the DEGAS 2 models of D_2 molecular dissociation and deuterium neutral transport, at least for the plasma conditions found in the main chamber of NSTX. Because we examine four H-mode shots, with minimal complications due to turbulent fluctuations, and because we have absolutely calibrated camera and gas puff data, this work represents the most comprehensive validation of DEGAS 2 for deuterium to date. The paper is organized as follows: Section 2 provides an introduction to the GPI diagnostic on NSTX, and Sec. 3 introduces DEGAS 2. Section 4 describes the relative comparison between DEGAS 2 and GPI, and Section 5 describes the absolute calibration of GPI camera and comparison with the DEGAS 2 simulations. Finally, in Sec. 6 we summarize and discuss the results.

2. GPI diagnostic in NSTX

A brief review of the gas-puff-imaging (GPI) diagnostic on NSTX is included here, more details can be found in Ref. [7–9]. The GPI measurement on NSTX is a two dimensional diagnostic of edge turbulence near the outer midplane. A gas puffing manifold with 30 holes of 1 mm diameter and 1 cm apart located at the outer wall behind projection of RF antenna introduces a deuterium gas puff into the plasma, and the visible line emission from this gas cloud is then imaged by a fast camera. Since the turbulence is highly elongated along the magnetic field, the D_α light from GPI gas puff cloud is viewed along the local magnetic field to resolve the smaller scale radial versus poloidal structure of turbulence.

Fig. 1(a) shows a schematic of GPI gas puff cloud and camera view along the magnetic field and Fig. 1(b) shows the location of GPI view, which is near the separatrix and about 20 cm above the mid-plane. The fast camera used on NSTX for this experiment took images at 397,660 frames per second and resolution of the optics was 64×80 pixels. This camera imaged the D_α light from the gas cloud through a 657 ± 5 nm filter (FWHM). The GPI gas puff increased the brightness of the D_α by about 20 times above the background, and thus localized the emission for improved spatial resolution. The spatial resolution of the optics is about 0.3 cm at the gas cloud.

The amount of light emitted in a spectral line in plasma associated with a radiative transition from neutral atom state p to state q depends on the neutral density and the local electron density and temperature through an expression of the form [10]:

$$S = n_0 f(n_e, T_e) A \qquad (1)$$

Here, n_0 is the local density of neutral ground state; A is the radiative decay rate of the transition from p to q. The function $f(n_e, T_e)$ is obtained from a collisional radiative model for the atom [10] and provides the ratio of the density of the upper state p to that of the ground state. Thus, the local D_α light emission rate should depend on the electron density and temperature as well as the neutral density, as previously discussed in [8-12].

3. DEGAS 2

DEGAS 2 simulates the transport of neutrals through plasma and vacuum using the Monte Carlo method [1, 10-12]. In these particular simulations, the 30 holes of the GPI gas manifold are represented as ten 2 x 2 cm squares aligned with the pitch of the actual manifold. The deuterium molecules are sampled randomly from a 300 K thermal energy and cosine angular distributions. As the molecules penetrate the plasma, they undergo ionization, dissociation, and elastic scattering; resulting molecular ions are assumed to be ionized, dissociated, or recombined immediately. Any product atoms are then tracked through the plasma and interact with it via ionization and charge exchange [10]. The particle track terminates upon ionization of the atom. Along the particles' paths, the volumetric source of D_α photons is accumulated in each computational zone. The view of the GPI camera is simulated by integrating through the simulation volume along a chord corresponding to each of the 80 x 64 pixels. Note that the neutral density profiles analyzed here are from the GPI gas puff and not from the background of D_α recycling light in the edge, which was too small to be measured accurately with the GPI camera at these high framing rates.

4. Comparison of DEGAS 2 and GPI

In this section we will present the measured 2-D profiles of the time-averaged D_α light emission from the GPI gas puff, and compare them with those obtained with the neutral transport simulation code DEGAS 2. Section 5 will describe the absolute calibration.

For this comparison, we use 4 shots taken on the same NSTX run day and also be used in [13], as listed in Table 1. All of these shots are H-mode discharges with considerable lithium coating with a toroidal magnetic field 4.3 KG and plasma current of 650-700 KA. The total size of the D_2 GPI gas puff was nominally the same for all shots, and measured to be 5.3±1 Torr-liters (about 1.7×10^{20} molecules) by the drop in plenum pressure after the puff.

The time evolution of the mean D_α light intensity from this GPI gas puff for each of these shots is shown by the black curves of Fig. 2. These curves come from averaging the total light in each GPI camera frame, taken at a rate of 397660 frames/sec. The gas was puffed into the steady-state part of the discharge at ~0.5 sec, and the D_α light from the puff is visible starting ~15 msec after the start of the gas puff. The gas puff light peaks ~30 msec after it starts, and then decays with a time constant of ~50 msec as the gas is exhausted from the manifold. The peak value of the GPI intensity is about the same for all shots, as expected from the similar gas puff levels. Also shown in Fig. 2 are the outer midplane separatrix position vs. time and the location of the radial peak of the GPI light, which are discussed at the end of this section.

The time periods used for comparing GPI and DEGAS 2 are shown by the gray shaded regions in Fig. 2. These were all 10 ms intervals near the peak of the GPI signal during which time there were no ELMs. The Thomson scattering electron density and temperature data taken at these times are shown in Fig. 3. These profiles were combined with magnetic equilibria computed with EFIT [14] to map the densities and temperatures along flux surfaces to provide the input plasma parameters for DEGAS 2.

Figures 4, 5, 6, and 7 show the 2-D comparisons of the D_α light emission from the GPI data with the D_α emission calculated from a DEGAS 2 simulation for the shots in Table 1. At the top of each figure, the color contours are from the simulation, where the units are W/m^2-sr, and the white contours are the 2-D GPI D_α emission profiles averaged over the 10 ms periods shown in Fig. 2. In each figure the local radial coordinate is approximately horizontal, the local poloidal coordinate is approximately vertical, the separatrix is shown by the black dashed line, the limiter (downstream RF antenna) is shown by the dotted red line, and the GPI gas manifold location is shown by the blue line.

At the bottom of each figure are the relative shapes of the radial distributions of the D_α light emission from both GPI and from DEGAS 2. These are found by separately integrating the GPI and DEGAS 2 contours (top) over the flux surface coordinate with respect to the separatrix, so that the area under each curve is the same for GPI and DEGAS 2 for all shots. The differences between the locations of the peaks in the radial

profiles of GPI and DEGAS 2 are listed in Table 1; for all cases these peak locations were within 0.2-1.4 cm with an uncertainty of about 0.3 cm. Also listed in Table 1 is the differences in the radial widths (FWHM) of these distributions for each shot; these range from 0.6 to 2.2 cm. Thus the relative shapes of 2-D emission profiles for D_α from DEGAS 2 and GPI results agree well, similar to earlier analyses for helium GPI in NSTX [12]. Also shown at the right of Table 1 are the ratios of the measured GPI light to the DEGAS 2 predicted D_α light within this field of view for the 10 msec period of interest for each shot, normalized so that this ratio is assumed to be 1.00 for #141324. These are all within 0.79-1.0, indicating that the ratio of the GPI/DEGAS 2 light intensity is fairly consistent from shot-to-shot in this database.

For comparison, we also used the KN1D code [15] to calculate the edge neutral density profiles and D_α light emission due to deuterium gas coming from the wall (e.g. due to recycling and outgassing), and not specifically from a GPI gas puff. KN1D is a kinetic transport code for simulating the penetration of atomic and molecular hydrogen into a ionizing plasma, utilizing in one spatial and two velocity dimensions. The Thomson scattering data of Fig. 3 for the electron density and temperature profiles are input to KN1D assuming that the ions and electrons have the same temperature. KN1D runs using the same T_e but different T_i show no significant differences. Figure 8 shows the radial location of the peak of the D_α light from GPI, DEGAS 2, and KN1D profiles in terms of the local electron density and temperature. In all cases, the peak of D_α profile is in the electron density range (1-5) $\times 10^{19}$ m^{-3} and between electron temperatures 10-100 eV. The GPI peaks have a wider range in T_e and n_e than the DEGAS 2 and KN1D simulations, most likely because the GPI signal is affected by fluctuations in the plasma parameters which are not accounted for in these simulations.

The electron temperatures at the emission peak locations are well above the 15~18eV for the simulations in [12], even though those experiments and simulations used helium, which has an ionization potential well above that of hydrogen. The deuterium gas penetrates further than helium due to efficient charge exchange with the main plasma ions, resulting in D temperatures that are a significant fraction of the ion temperature. A higher starting energy for the D atoms, that coming from dissociation, also plays a role.

The small differences between the observed and calculated D_α profiles of Figs. 4-7 can be attributed to uncertainties in the assumed density and electron temperature profiles at the GPI puff location. These uncertainties could be due to small (~1 cm) variations in the separatrix location during the time of interest, or to small-scale turbulent fluctuations seen by the Thomson scattering which are not apparent at the GPI location or to uncertainties in the mapping of the midplane flux surfaces to the GPI location above the midplane. Thus the results of Figs. 4-7 and Table 1 can be considered a successful validation of the DEGAS 2 code with the GPI data, to within the uncertainties of the experimental data.

Finally, it is interesting to compare the radial locations of the peak in the measured D_α profile with the separatrix locations over longer periods of time, as was shown in Fig. 2. For that figure the peak in the poloidally-averaged GPI light was mapped to the outer midplane using EFIT, and then plotted along with the outer midplane separatrix from EFIT. The peak of the D_α light was almost always within ±1-2 cm of the separatrix for for all times, even for the ~15 msec periods before the GPI puff, except during ELMs when the GPI light suddenly moves outward [16]. This suggests that the comparisons of Fig. 4-7 are at least qualitatively similar at other times during these shots, and that the GPI gas puff is not significantly perturbing the local plasma parameters during the puff.

5. Absolute calibration for shot #141324

We have performed an optical calibration to find the absolute value of the number of D_α photons emitted per D atom injected from the GPI gas puff as viewed by the GPI camera in order to compare this number with that computed by DEGAS 2. The experimental calibration was made with a white light calibration lamp (Optronic Laboratories Model 420), which had a spectral radiance at 650 nm (near D_α) of 1.02×10^{-7} (W/sr cm^2 nm). The entire GPI optical system including the front-end mirror and lenses, fiber bundle, D_α filter, and camera (except for the vacuum window) were removed from NSTX and set up to view this calibration lamp. Since the D_α filter had a calibrated FWHM of ~10 nm±1 nm, the irradiance of this lamp as viewed by the GPI optics was

$1.3\pm0.2 \times 10^{-5}$ (W/cm^2), where the lamp emission was integrated over 4π sr. One pixel in the center of the image of the lamp had a time-averaged camera signal of 639 counts (±5%) at an exposure time of camera of 41,000 μs. Thus the absolute response of the camera to a source D_α light was 0.016 counts/(μs-pixel) for a source of 1.3×10^{-5} W/cm^2. Since each D_α photon has an energy of 1.9 eV, this implies 1 count/(μsec-pixel) corresponds to 2.7×10^{15} photons·μsec/cm^2–sec. The vacuum window transmission was measured to be 0.88 after the run. Thus, the absolute response of the camera to a D_α light source is 1 count/(μsec-pixel) for 3.1×10^{15} photons·μs /cm^2–sec, with an uncertainty of about ±20%. Note that this calibration is independent of the distance of the source from the camera (this arrangement was slightly different from the one in NSTX), since the calibration pixel was chosen to be in the center of the lamp window, and the radiance is independent of the distance from the source to the lamp.

For the GPI data use in this paper, the exposure time of the camera was 2.1 μs, and the total area viewed at the plane of the gas puff cloud was ~560 cm^2. Thus, a camera response of 1 count/pixel at this exposure time in this field of view should correspond to (3.1×10^{15} photons·μsec /cm^2–sec)(560 cm^2)/(2.1 μsec) ~ 8.2×10^{17} photons/sec. The average number of counts per pixel in the frames measured in shot 141324 is ~4.8 counts·sec/pixel, averaged over a gas puffing time of 60 msec. Thus the total number of photons emitted during this gas puff in this field of view for this shot is (8.2×10^{17}photons/sec)(4.8 counts/pixel) = 3.9×10^{18} photons of D_α, with an uncertainty of about ±20%.

The total number of deuterium gas atoms puffed during this shot was measured by the pressure rise in the vessel without a shot (without pumping), and by the drop in pressure in the gas plenum, to be 5.3 Torr-liters or 3.5×10^{20} atoms, with an uncertainty of about ±10%. Thus, the absolutely calibrated number of photons emitted per D atom within the GPI field of view in this shot was (3.9×10^{18} photons/3.5x10^{20} atoms) ~ 1/89, with an uncertainty of about ±25% from both the photons and atoms measurements.

The number of photons in the DEGAS 2 simulated GPI image of shot #141324 (Fig. 6) was 1.1^{16} photons/s assuming a total D source rate of 8.2^{17}, yielding a ratio of 1/75

photons/ionization, very close to the experimental value. On the other hand, this is considerably smaller than the ratio of 1/15 expected from the atomic physics models [17, 18]. The apparent discrepancy is due to the fact that the simulated camera sees only about half of the total photon emission from the GPI gas puff, and that roughly half of the puffed atoms travel vertically outside the problem boundary without emitting photons. To examine sensitivity of the simulations to the location of these boundaries, we repeated the run of shot #141324 with a domain 50% larger in the vertical direction. There was no apparent effect on the simulated camera image; the number of photons in the image increased by only 3%.

In conclusion, for the chosen shot #141324, the camera calibration produced an estimate of 1/89 D_α photons per injected gas atom, with an uncertainty of ±25%, and the DEGAS 2 model produced an estimated 1/75 D_α photons per injected gas atom. Thus, we conclude that GPI and DEGAS 2 agreed to well within a factor-of-two in the absolute number of D_α photons per injected gas atom. The relative ratio of GPI to DEGAS 2 light emission for the other three shots (see Table 1) were within about 20% of that for #141324 so that this statement applies to all four shots considered here

6. Summary

This paper presents the results from GPI experiment and DEGAS 2 simulation, that this provide the best comparison of the GPI measurement with DEGAS 2 simulation so far made. From the comparison between GPI and DEGAS 2, they are matched to within the estimated uncertainties. We also have done an absolute calibration of the GPI light level, and the results agree with DEGAS 2 within a factor of 2. We have compared the peak location of D_α light. From both the results of experiments and simulations, the peak of D_α profile always appeared at range of electron density of $(1\text{-}5)\times10^{19}$ m^{-3} and electron temperature of 10-100 eV.

Acknowledgments

The authors wish to thank B. LaBombard of MIT and B. Davis of PPPL for the help with KN1D, R.J. Maqueda for taking the GPI data used in this experiment, F. Scotti of PPPL for the help with the calibration of the GPI camera. One of us (Bin Cao) thanks the NSTX team for support during his visit to PPPL. This research was funded by National Nature Science Foundation of China under Contract No. 11021565 and US DOE Contract DE-AC02-09CH11466.

References

[1] http://w3.pppl.gov/degas2/

[2] P. Helander, T. Fulop, and P.J. Catto, Phys. Plasma, **10,** 4396 (2003)

[3] R. D. Bengtson, P. M. Valanju, A. Ouroua, and W. L. Rowan, Rev. Sci. Instrum, **61** (1990)

[4] R.L. Boivin et al, Rev. Sci. Inst. **72**, 961 (2001)

[5] J. Harhausen, A. Kallenbach, C. Fuchs, Plasma Phys. Control. Fusion **53** 025002 (2011)

[6] P. W. Ross, "Ion Power Balance in Neutral Beam Heated Discharges on the National Spherical Torus Experiment (NSTX)", Ph.D. thesis, Princeton University (2010)

[7] R.J. Maqueda et al, Rev. Sci. Inst. **72**, 931 (2003)

[8] S.J. Zweben et al, Phys. Plasmas **9**, 1981 (2002)

[9] S.J. Zweben et al, Nucl. Fusion **44**, 134 (2004)

[10] D.P. Stotler, B. LaBombard, J.L. Terry, S.J. Zweben, J. Nucl. Mater, **313-316** (2003) 1066

[11] D.P. Stotler, D.A. D'Ippolito, B. LeBlanc, R.J. Maqueda, J.R. Myra, S.A. Sabbagh, and S.J. Zweben, Contib. Plasma Phys., **44** (2004) 294

[12] D.P. Stotler, J.Boedo, B. LeBlance, R.J. Maqueda, S.J. Stewart, J. Nucl. Mater. **363-365** (2007) 686

[13] B. Cao, S. Zweben, D. Stotler, M. Bell, A. Diallo, S. Kaye, and B. LeBlanc, **54** (2012)

[14] L. Lao et al, Nucl. Fusion **25** (1985) 1611

[15] http://www.psfc.mit.edu/~labombard/KN1D_Source_Info.html

[16] R.J. Maqueda et al, Phys. Plasmas **16** (2009) 056117

[17] L. Johnson and I. Hinov, J. Quant. Spectrosc. Radiat. Transfer Vol. 13 (1973) 33

[18] S. D. Loch, C. P. Balance, M. S. Pindzola, and D. P. Stotler, Plasma Phys. Control. Fusion 51 (2009) 105006

Table 1 - Shot list, plasma parameters, and comparison between GPI and DEGAS 2

shot	Start time (ms)	P_{NBI} (MW)	n_e (10^{13} cm^{-2})	I_p (KA)	B (kG)	Total gas puff (Torr−liters)	GPI-DEGAS 2 Peak difference (cm)	GPI-DEGAS 2 Width difference (cm)	GPI-DEGAS 2 intensity ratio
141307	480	3.8	7.5	700	4.43	5.2	0.40	0.8	0.90
141320	530	4.0	8	650	4.43	5.3	0.40	2.2	0.79
141322	530	4.0	8	650	4.43	5.4	1.20	0.8	0.93
141324	530	2.9	6	650	4.43	5.3	0.20	0.6	1.00

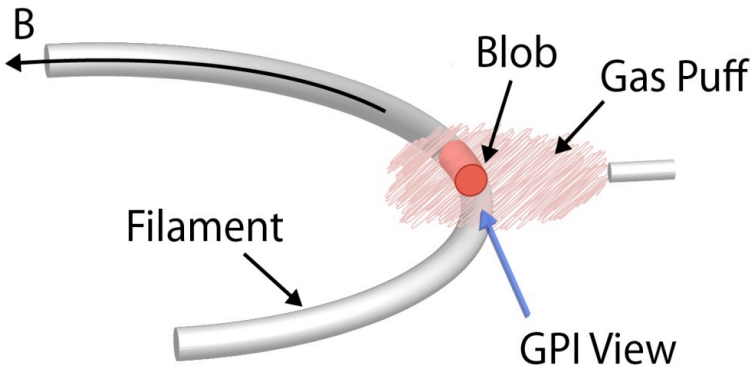

(a)

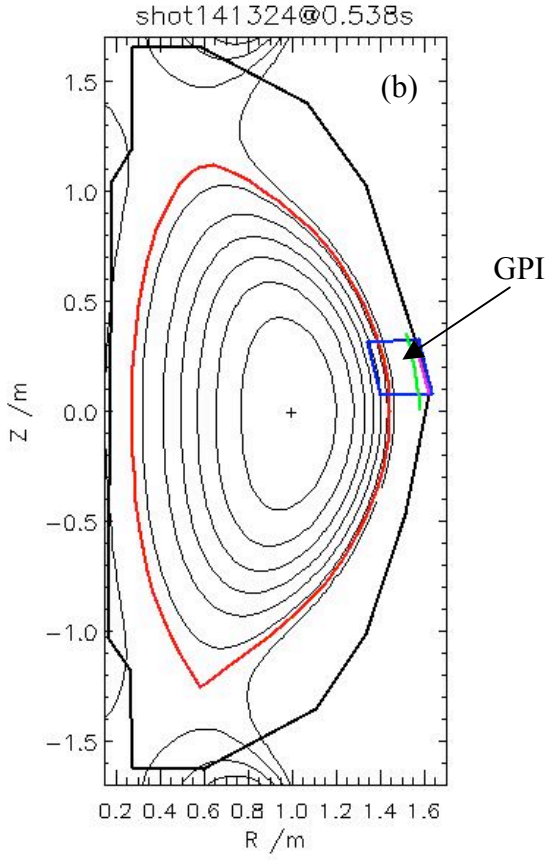

Fig. 1 Schematic of the GPI diagnostic geometry (top), and the location of GPI diagnostic in NSTX (bottom). The GPI fast camera views the D_α light emitted from gas puff cloud along the local magnetic field direction. The red line is the separatrix, the blue line is GPI viewing area, the green line is the RF limiter shadow, and the pink line is the gas puff manifold.

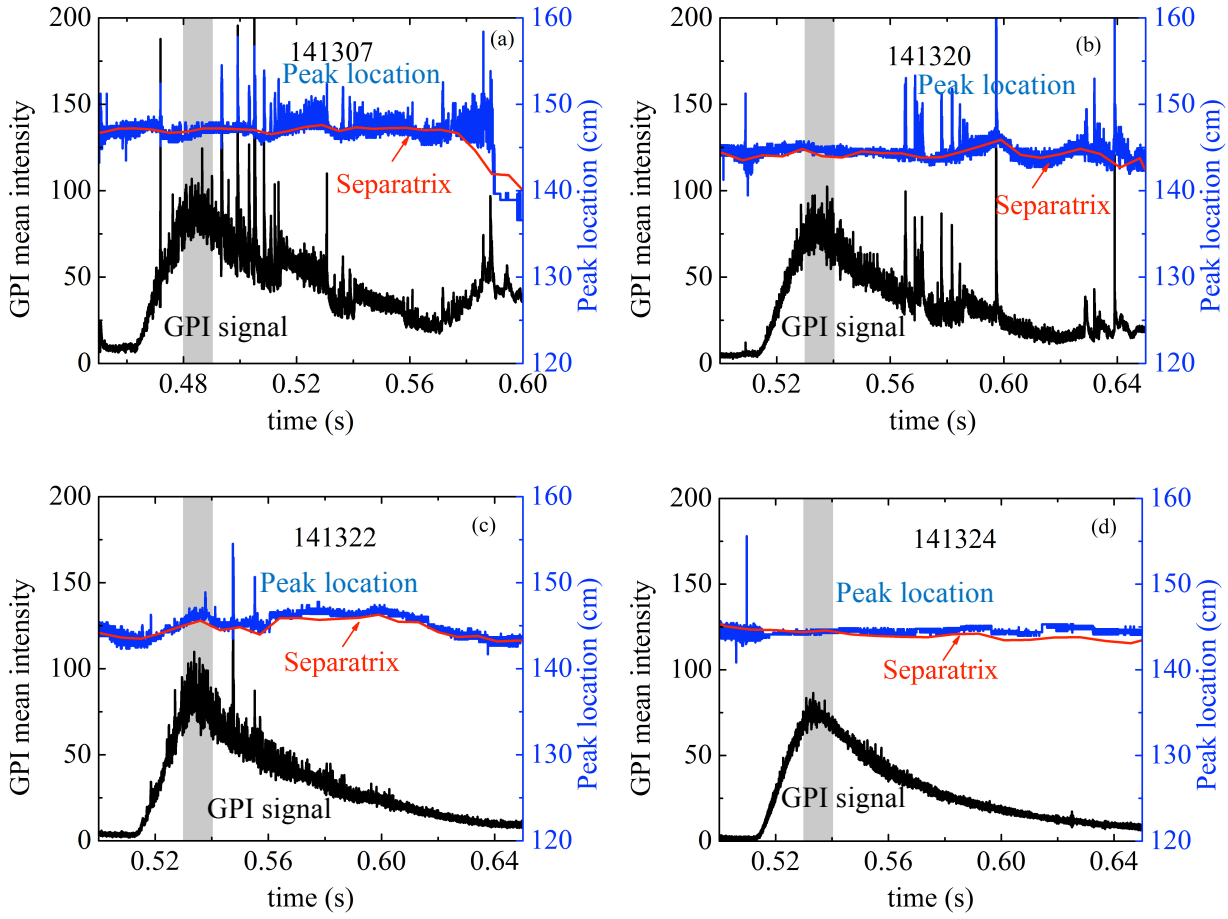

Fig. 2 Time dependence of mean GPI intensity and peak location mapped to the outer midplane. The GPI puff begins to be visible ~15 msec after the start of these traces. The gray area is the time region used in this paper, and the separatrix location at the outer midplane is also shown.

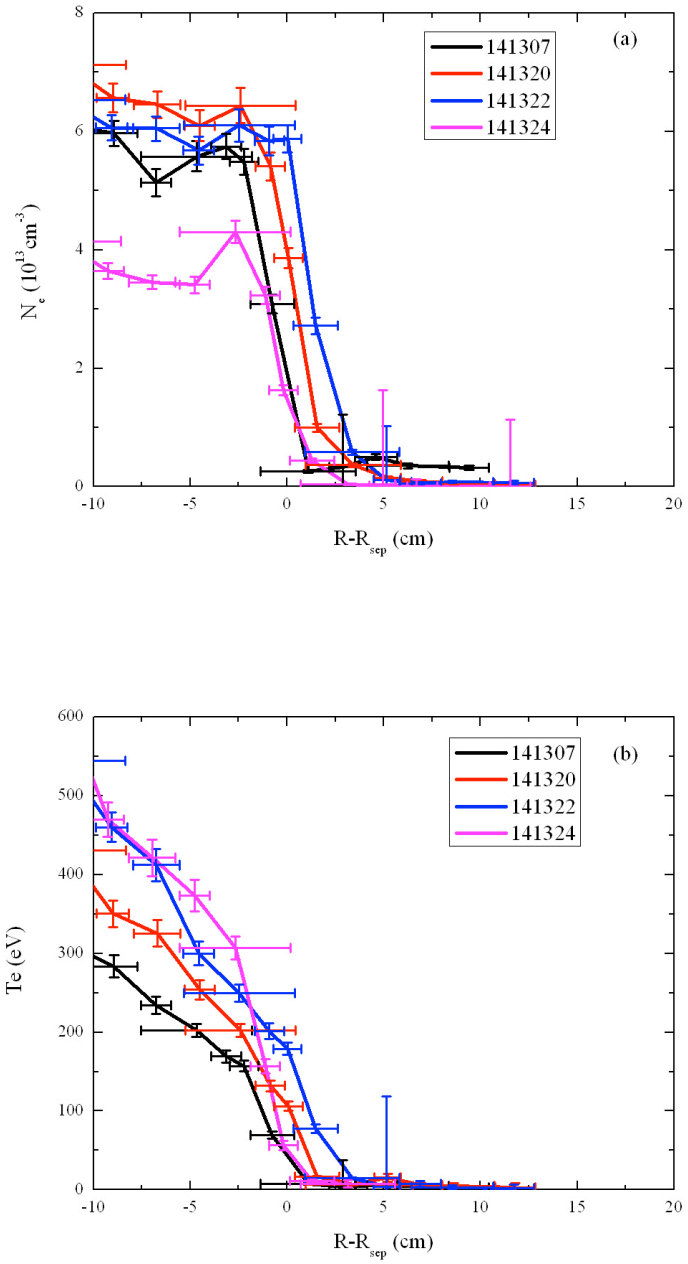

Fig. 3 Radial profiles from the Thomson scattering diagnostic for (a) the electron density and (b) the electron temperature relative to the separatrix location for the shots and times in Table 1. The GPI field of view is normally in the vicinity of the separatrix.

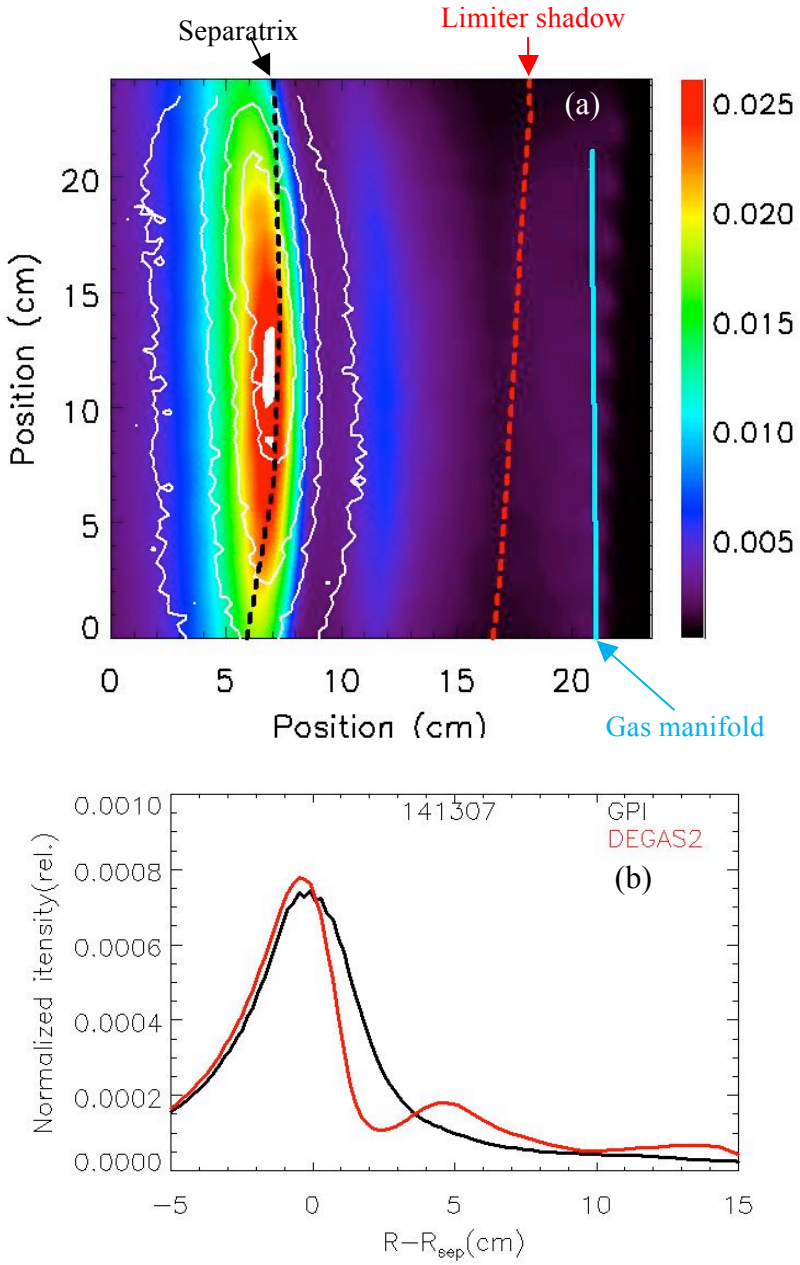

Fig. 4 Comparison between the D_α light emission from DEGAS 2 and GPI data for #141307. In figure (a) the color contours are the DEGAS 2 results in units of W/(m^{2}sr), the white contours are the GPI results, the black dash line is the separatrix, the red dash line is the limiter shadow, the blue line is the gas manifold. In (b) are the radial profiles of the relative shapes of the D_α light emission mapped with respect to the outer midplane separatrix, all the curves are normalized to have the same area.

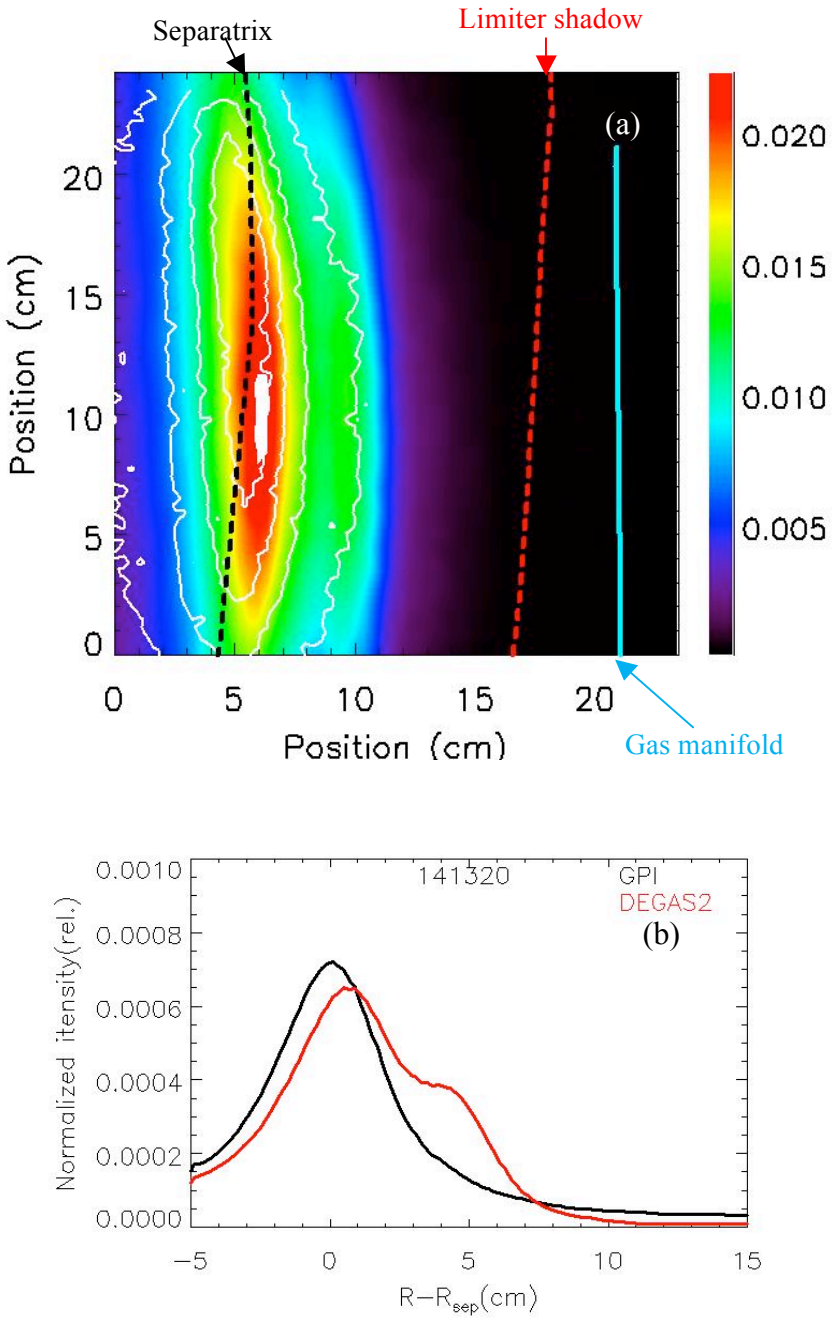

Fig. 5 Comparison between the D_α light emission from DEGAS 2 and GPI data for #141320. In figure (a) the color contours are the DEGAS 2 results in units of W/(m^{2}sr), the white contours are the GPI results, the black dash line is the separatrix, the red dash line is the limiter shadow, the blue line is the gas manifold. In (b) are the radial profiles of the relative shapes of the D_α light emission mapped with respect to the outer midplane separatrix, all the curves are normalized to have the same area.

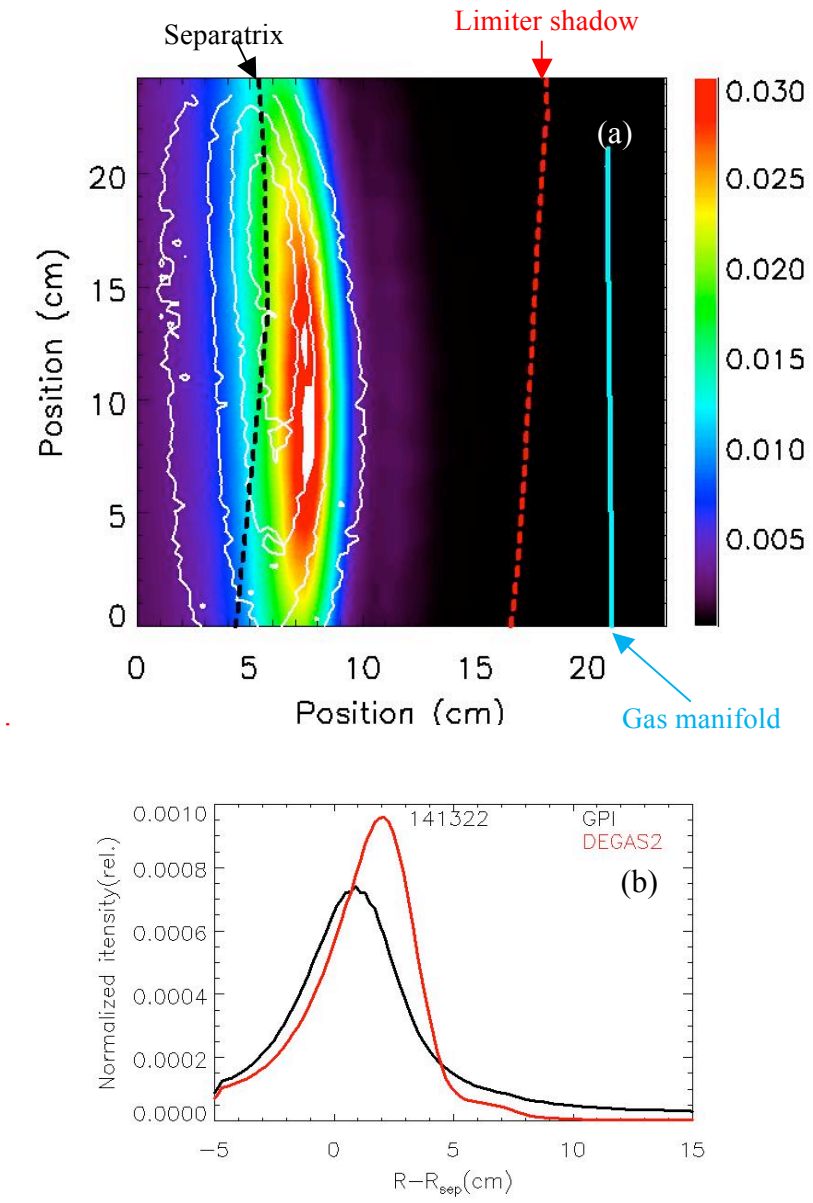

Fig. 6 Comparison between the D_α light emission from DEGAS 2 and GPI data for #141322. In figure (a) the color contours are the DEGAS 2 results in units of Wa/(m^2sr), the white contours are the GPI results, the black dash line is the separatrix, the red dash line is the limiter shadow, the blue line is the gas manifold. In (b) are the radial profiles of the relative shapes of the D_α light emission mapped with respect to the outer midplane separatrix, all the curves are normalized to have the same area.

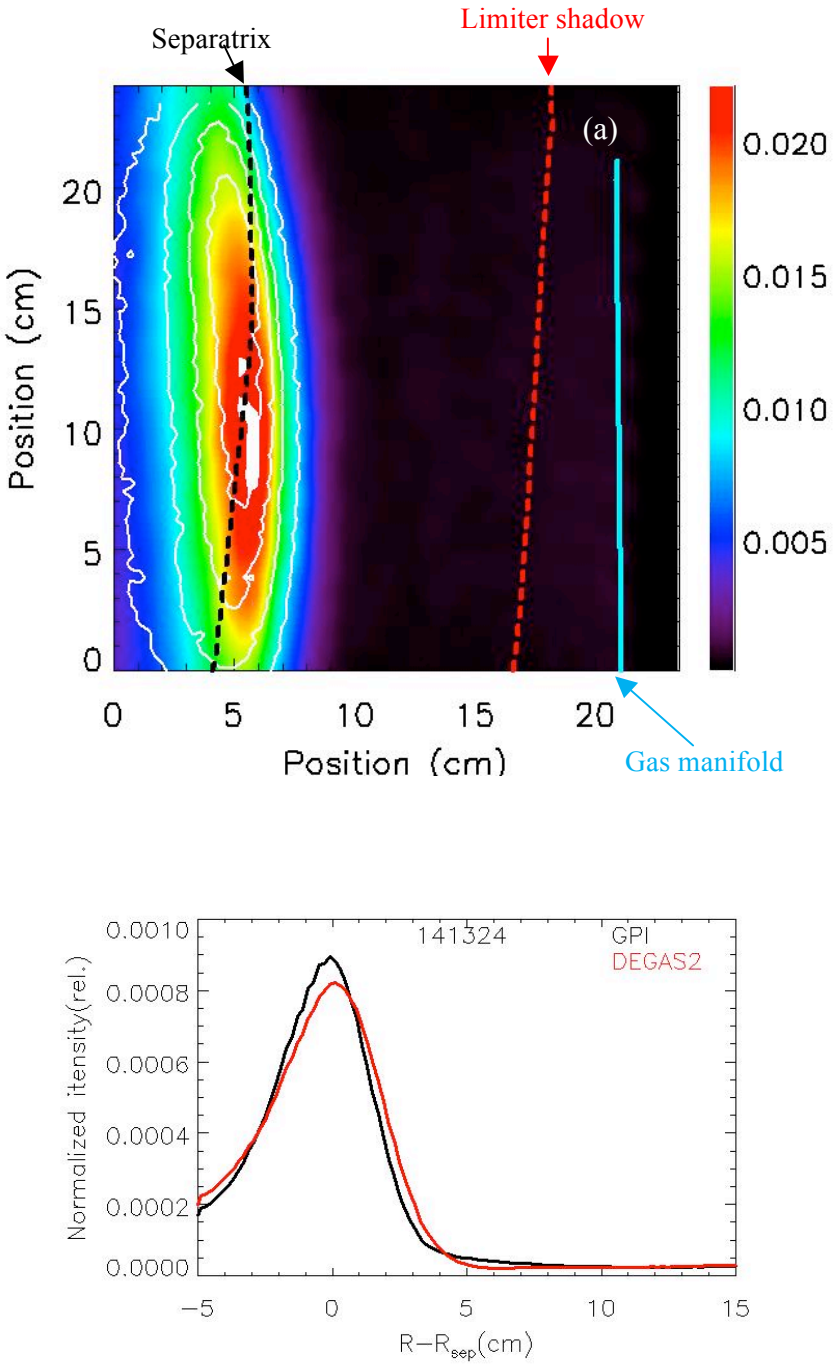

Fig. 7 Comparison between the D_α light emission from DEGAS 2 and GPI data for #141324. In figure (a) the color contours are the DEGAS 2 results in units of Wa/(m^2sr), the white contours are the GPI results, the black dash line is the separatrix, the red dash line is the limiter shadow, the blue line is the gas manifold. In (b) are the radial profiles of the relative shapes of the D_α light emission mapped with respect to the outer midplane separatrix, all the curves are normalized to have the same area.

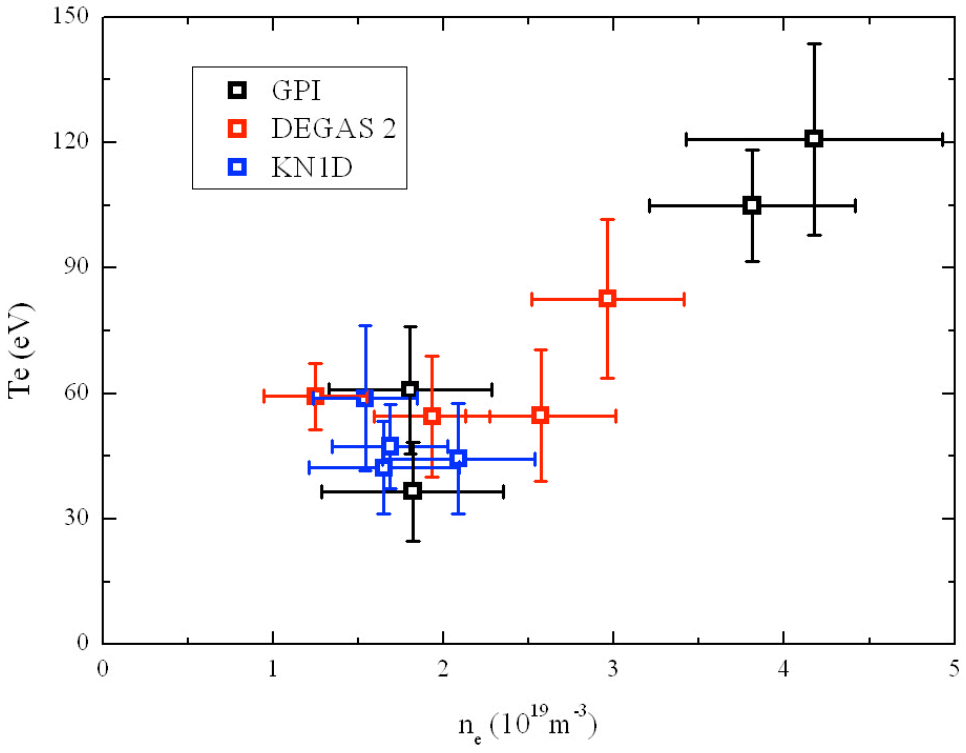

Fig. 8 Electron density and temperature at the peak location of D_α light from GPI, DEGAS 2 and KN1D. The DEGAS 2 and KN1D modeling used Thomson scattering data as input electron density and temperature profiles, and assumed $T_i=T_e$. The GPI data is averaged over 10 msec. The peak of D-alpha light almost always appeared in the regions at T_e =10-100 eV and n=(1-5)x10^{19} m^{-3}

The Princeton Plasma Physics Laboratory is operated
by Princeton University under contract
with the U.S. Department of Energy.

Information Services
Princeton Plasma Physics Laboratory
P.O. Box 451
Princeton, NJ 08543

Phone: 609-243-2245
Fax: 609-243-2751
e-mail: pppl_info@pppl.gov
Internet Address: http://www.pppl.gov